Towards integrated multi-sensor platform using dual electrochemical and optical detection for on-site pollutant detection in water

Fadhila Sekli-Belaidi, Léa Farouil, Ludovic Salvagnac, Pierre Temple-Boyer, Isabelle Séguy, Jean-Louis Heully, Fabienne Alary, Eléna Bedel-Pereira, Jérôme Launay

Towards integrated multi-sensor platform using dual electrochemical and optical detection for on-site pollutant detection in water

F. Sekli Belaïdi [a,b], L. Farouil [a,b], L. Salvagnac [a,b],

P. Temple-Boyer [a,b,†], I. Séguy [a,b,‡], J.L. Heully [c], F. Alary [c], E. Bedel-Pereira [a,b,§], J. Launay[a,b,*]

[a] CNRS, LAAS, 7 avenue du colonel Roche, F-31400 Toulouse, France

[b] Université de Toulouse, UPS, LAAS, F-31400 Toulouse, France

[c] LCPQ-IRSAMC, Université de Toulouse, 118 route de Narbonne, F-31062 Toulouse, France

Corresponding author*: jlaunay@laas.fr, tel: +33561336809

[†]temple@laas.fr, [‡]seguy@laas.fr, [§]elena@laas.fr

Abstract

The present work is dedicated to the development of a lab-on-chip (LOC) device for water toxicity environmental analysis and more especially herbicide detection. The final goal is focused on the functional integration of three-electrode electrochemical microcells (ElecCell) and organic photodetectors (OPD) in order to perform simultaneously electrochemical and optical detection in the frame of algal metabolism monitoring. Considering three different algae, i.e. *Chlamydomonas reinhardtii*, *Pseudokirchneriella subcapitata* and *Chlorella vulgaris* while dealing with photosynthesis, the multi-microsensor platform enables to measure the variations of microalgae fluorescence as well as oxygen production. It is applied to study the Diuron herbicide influences on algal metabolism, evidencing fluorescence enhancement and oxygen production inhibition for concentrations as low as few tens of nanomoles. These results are performed with unconcentrated and six time concentrated algae solutions respectively, to estimate the ability of this dual-sensor system to conduct measurements without any sample preparation. Thus, according to the obtained results, the proposed LOC device is fully adapted to the electrochemical/optical dual detection for on-site pollutant analysis, i.e. without sample pre-treatment.

Keywords

Compact fluidic platform, LED excitation, electrochemical detection, organic photo-detection.algal metabolism, herbicide detection.

1. Introduction

The effective management of water requires regular and continuous monitoring of quality to detect pollutants (nutrients, pesticides, and heavy metals) in order to prevent a serious threat to human health. Traditional monitoring techniques are generally based on laboratory analyzes of representative field-collected samples leading to considerable expenses. In addition, the standard available equipments are not portable. Therefore, the sample has to be collected directly on-site and even if best available transportation practices are applied, e.g. freezing the samples, the composition could change during the drive to the lab producing false outcomes. Indeed, in large part, the quality of the analysis results is determined by the integrity of the samples sent to the laboratory. In this context, portable lab-on-chip (LOC) monitoring systems seem well suited to offer an attractive alternative way to proceed among the analytical methods actually available. Even, if care must be taken to protect samples from contamination or tampering, in situ measurement avoids those high risks. Otherwise, they save time, reduce reagent volume and cost. In fact, only samples showing too high level of contaminants should be carried and analyzed through classical laboratory tools to determine precisely the composition of the sample.

Over the two last decades numerous papers have been published on integrated LOC devices developed, highlighting the efforts made and still to be done to reach real environmental applications. A. Jang *et al*. (2017*)*, who detail the 1986–2010 state-of-the-art of lab-on-chip sensors for environmental water monitoring, conclude that the environmental monitoring sensor systems commercially available are either prohibitively costly or highly inflexible. They use invasive sampling that can alter chemical and biological conditions at the observation site; or they have electrodes that must be dipped into the water containing the pollutants. They propose an array of LOC incorporated into an automated analyzer with customized user interface to perform the continuous measurement for on-site applications. They convert a biochemical phenomenon into a detectable and measurable electrical signal proportional to the analyte concentration. Among papers cited by Jang *et al*. (2017), Brayner *et al*. (2011) show that whole cell biosensors and bioassays are a good candidate solution to satisfy the implemented requirements. More particularly, Fernandez-Jaramillo *et al*. (2012) give a review of general knowledge of real time measurements and provide the necessary information to develop novel and custom biosensors for chlorophyll fluorescence measurement. They also emphasize that, as electronic devices are constantly evolving and becoming more efficient, equipments for measuring chlorophyll fluorescence will improve constantly in the same way. Indeed, various innovative and futuristic technologies have been developed between 2010 and 2015; Arduini *et al*. (2017) propose an exhaustive analysis of the literature of these

technologies very useful for (bio)sensor effective environmental applications. Moreover, in this context, micro- and nano-fabrication technologies permit microsystems development including all components on board of the chip like LOC structure that could be an early and rapid warning system for on-site detection.

Very recently, Tahirbegi *et al*. (2017) report a miniaturized microfluidic device with integrated optical measurements for the *in situ* detection of pesticides by monitoring the metabolism of algae *Chlamydomonas reinhardtii*. This system uses three external optoelectronic instruments positioned on the bottom of the glass chip to measure dissolved oxygen O_2, pH and algae fluorescence. Such a hybrid system will minimize the plug-and-play properties of this tool and the use of commercial components prevent to move towards flexible and tailor-made sensing systems. However, in order to deal with selectivity, beyond the use of several micro-algae, the combination of optical and electrochemical methods is very promising. Indeed, both detection principles are adapted to the analysis of biometabolims (for example through the mesaurement of dissolved oxygen concentration and pH) but are concerned by different interferents. As a result, together, they can cope more easily with water sample complexity in the frame of water pollution

The present work is focused on the one hand, on the electrochemical and fluidic improvements in order to simplify the first hybrid biosensor LOC prototype (Tsopela 2014, 2016) (Sekli Belaidi 2016), which we have proposed. On the other hand, for further integration of optical transducers (dedicated to dual detection), we developed an organic photodiode (OPD) to measure the variations of the microalgae fluorescence. To evaluate performances of the whole tool, three green micro-algae strains are chosen as the biological sensing element*: Chlamydomonas reinhardtii* (Cr) for the electrochemical part, plus *Pseudokirchneriella subcapitata,* (Ps) and *Chlorella vulgaris* (Cv) for the optical one. Different media, with concentrated or un-concentrated algae solution, are prepared with toxic substances in order to study and to compare both electrochemical and optoelectronic sensors responses.

This paper demonstrates the utility of a standard multi-sensors platform using together the physical principles of electrochemistry and optic in a microfluidic system to allow fast and simple on-site complementary measurements for environmental applications. The different elements (fluidic structure with multi-channel for measurements, emission/reception with the optical devices, autonomous electrochemical microcells) are optimized, fabricated, tested and partially integrated on a unique platform. These dual-sensors allow the dual detection of chemical pollutants (pesticides) in fresh water thanks to the use of green micro-algae directly, with no added chemicals. This study is focused on the effects of Diuron herbicide on algae in order to compare the two aforementioned sensors characteristics. Indeed, Diuron is well known to enhance algae fluorescence and is often considered as a model pollutant for sensitivity qualification in a variety of detection platforms using algae as biosensors (Vedrine 2003). The advantages of each kind of detection (electrochemical versus optical) are discussed in relation with the final application, which is the on-site detection of fresh water with no pretreatment.

2. Material and methods

2.1. Design of the lab-on-chip

The LOC platform considered here, consists in fluidic chambers integrating electrochemical sensors (in-situ) and chambers dedicated to optical fluorescence-based detection with optical devices stuck on the two sides of the chip. Our previous work had consisted in the validation of the electrochemical sensor (Tsopela 2014, 2016) (Sekli Belaidi 2016) on a first prototype. Here, our efforts carry the validation of the optical sensor of an LOC whose fluidic is optimized. The new fluidic system is designed in order to ameliorate liquid injection, cleaning protocols and to reduce costs thanks to, among others, the use of dry film resists (DFR) instead of the SU-8 photoresist used in previous LOC, (Tsopela 2016). The working electrodes have been hollowed out to make it semi-transparent to enhance light harvesting into the fluidic chamber and algae photosynthesis detection near the electrochemical sensor. Light emitting diodes (LED) and an organic photodiode (OPD) are disposed on each side of the fluidic chamber. The LED role consists in stimulating the algae (470 nm maximum emission is in accordance with green algae absorbance) to trigger the photosynthetic activity, responsible for oxygen and fluorescence production. The OPD constitutes another part of the optical detection system, which also includes excitation and detection filters. So, reliable optical sensing integration, i.e. without any device ageing, constitutes a very challenging step for those microsystems. Previously, electrochemical sensing experiments were successfully conducted with blue organic light emitting diodes (OLED) as light source (Tsopela 2016). However, their efficiency could be quite not sufficient to ensure optical sensor reliability and repeatability since more light intensity is needed for algae fluorescence than for photosynthesis. Moreover, stable excitation filters, easy to integrate, represent another issue that we are currently addressing by developing micro-cavity OLED. So, at this stage of the study, integration will be confined to the detection part of the optical sensor, i.e. the photodiode and detection filter. The structure of the LOCs is shown in Fig.1.

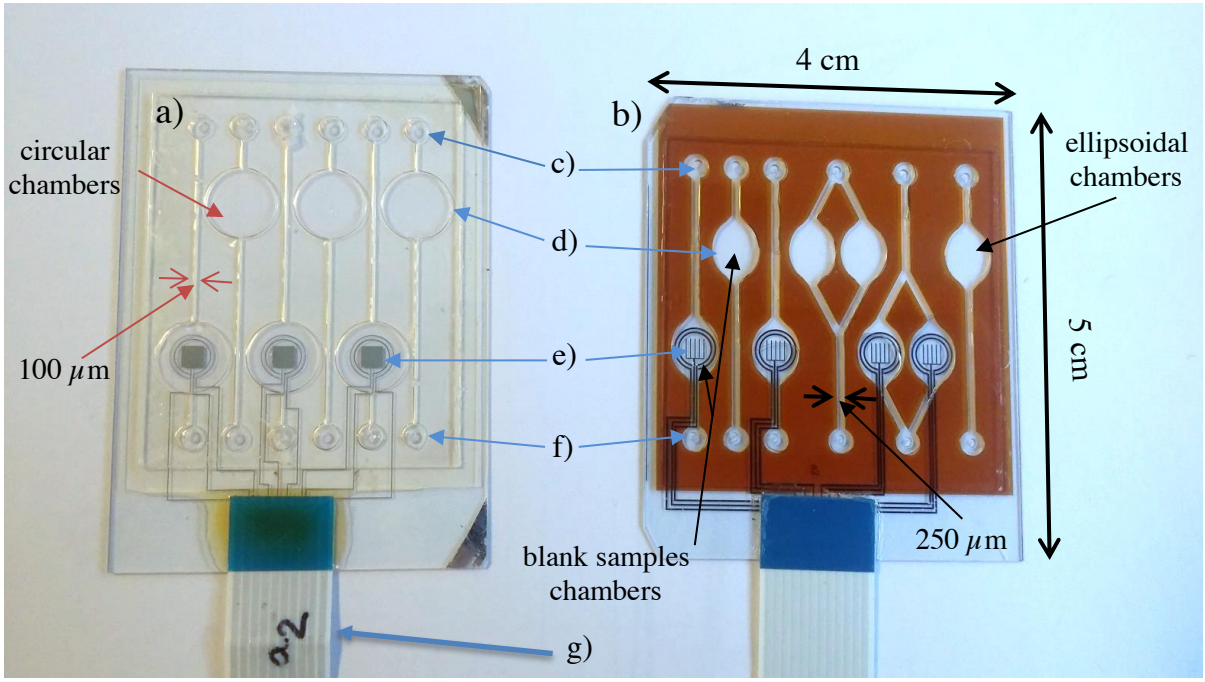

Figure 1: Sensors platform obtained after packaging: a) First generation structure SU8-LOC, b) New structure DFR-LOC, c) Inlet, d) Optical chamber, e) Electrochemical chamber, f) Outlet, g) Electrical connections.

2.2. Micro-fabrication of the lab-on chip

To begin the LOC fabrication process, the glass substrates are treated with oxygen plasma (800 W, 15 min) to enhance metal adhesion. Titanium and platinum films (thickness: 12 nm and 120 nm respectively) are then sequentially thermally evaporated under vacuum ($P < 10^{-6}$ mbar) and patterned using a bilayer lift-off process. Afterward, to define the electrochemical microcell (ElecCell) including the working ultra-micro-electrodes (UME) array surrounded by the counter and reference electrodes, as well as the pads for electrical connection to the external devices, a sturdy and stable silicon nitride (Si_3N_4) insulation layer (thickness: 100 nm) is deposited by low temperature inductively-coupled plasma-enhanced chemical vapor deposition (IC-PECVD) (Vanhove 2013). In the second phase of the LOC preparation, i.e. the fluidic system, SU-8 photoresist is replaced by DFR, a negative dry film resist, DF 1050 (from EMS Adhesives). It consists in a 50 µm photosensitive layer laminated through a hot-roll laminator (Dynachem 350 HR Laminator) with selected speed 0.5 $m.min^{-1}$, temperature 100°C, and pressure 2.5 bars. Despite its advantages (simple, fast and cheaper alternative to SU-8), the adhesion of DFR to the underlying wafer surface is of central importance for the durability of the patterned microfluidic system. In fact, delamination could be a catastrophic failure strongly depending on adhesion of the DFR film to the substrate. In order to enhance the adhesion to the under-laying Si_3N_4 film, a self-assembled monolayer (SAM) has been processed by immersion of the wafer into a mixture of 3-glycidyloxypropyl trimethoxysilane adhesion promoter using "CO_2 supercritic" thermodynamic conditions (60°C, 120 bars). After this silanization step, the wafer is rinsed with ethanol, dried at 110°C

for 3 minutes and cleaned by the use of a 800 W oxygen plasma process just before lamination. Then, lamination is repeated five times to obtain the 250 μm resist thickness. Next, the resist is exposed to 240 mJ.cm^{-2} UV light using a mask aligner followed by a post exposure bake (PEB) at 100°C for 15 minutes to obtain the fluidic structure. Finally, the resist is developed for 40 minutes in a commercially available cyclohexanon solution and the wafer is rinsed with deionized water and dried. At last, LOC cover is bonded and packaged according to the process defined by Tsopela *et al*. (2016).

This new fluidic structure, called DFR-LOC, provides a multiparameter measurement tool using a unique chip with the complete electrochemical cells integrated in three of the chambers while the three others are dedicated to the fluorescence-based optical detection (see Fig.1).

2.3. Electrochemical sensor

In electrochemical sensing, the measured current is directly related to the concentration of the monitored specific specie in the tested liquid, by tuning the voltage value corresponding to the chemical reaction (oxidation or reduction) to be observed on the working electrode. The three-electrode electrochemical microcell (ElecCell) devices have been designed to avoid any current through the reference electrode: the working electrode is polarized thanks to the reference one and the current due to the oxidative/reduction reactions is collected through a counter electrode. The three metallic electrodes are prepared under vacuum by physical vapor deposition before the fluidic micro-fabrication process (Tsopela 2016). Platinum or gold layers are deposited to create working and counter micro-electrodes respectively while silver layer constitute the reference one. However, silver films obtained by evaporation techniques are thin (few hundreds of nanometers), thus fragile. Therefore, specific attention is required during the steps of the fluidic fabrication process (such as cleaning process using oxygen plasma which could irreversibly damage the silver layer, or during the Si_3N_4 deposition). Moreover, knowing that the reference electrode stability is directly related to the metal layer thickness, it is impossible to achieve stability with evaporated thin films. Furthermore, one of the advantages of DFR-LOC platform, compared to the SU8 one, is to allow performing different post process functionalization, like silver electroplating which will ensure a thick layer for the future reference electrode.

In the present study, the silver/silver chloride (Ag/AgCl) reference electrode is prepared after the fluidic network fabrication by electrodeposited silver and subsequent partial transformation to silver chloride. The platinum (see section 2.2) is first preconditioned with an electrochemical protocol in sulfuric acid to improve adhesion and homogeneous deposition. The silver electroplating on platinum surface is accomplished from 0.3 M $AgNO_3$ in 1 M NH_4OH. The silver is deposited with a bias fixed at -20 mV versus Ag/AgCl/ Sat. KCl reference electrode at room temperature for 180 seconds and partially transformed to silver chloride in 1 M KCl solution by slow linear voltammetry at room temperature. The bias varies between 0.1 to 0.25V vs. Ag/AgCl/Sat. KCl reference electrode with a speed fixed at 1 mV/s. SEM images of this electrode are shown in Figure S1(a) (Supplementary information). The silver chloride, about 4 μm thick, consists in homogenous grains with a size ranging from one to two micrometers.

Even though silver chloride is often treated as an insoluble salt, it exhibits significant solubility in situations where the reference electrode is used for long-time applications. The dominating ageing factor is the complexation of silver chloride in the presence of chloride ions. In our case, long-time stability in an electrolyte with 0.1 M chloride ions is verified for several hours (see Fig. S1(b) in Supplementary information). It emphasizes that the electrodeposited AgCl is thick enough to provide a stable reference electrode for our application. In the same way, we optimize the detection properties of the working electrodes by post-process black-platinum (PtBl) deposited on platinum layers to obtain finally a three dimensions porous UME (Tsopela 2014).

24. Optical sensor

As mentioned above, the optical sensor is made up of four independent elements: a LED, two optical filters and an OPD. The purpose of these filters is respectively to avoid overlaying of LED spurious emission (see Fig. S2 supporting information) and algae fluorescence signal, and to prevent excitation light to reach the OPD. The optical excitation includes a commercial blue LED (KP-3216QBC-D from Kingbright) and an excitation filter (ET470/40x from Chroma Technology Corp). On the over side of the fluidic platform, the integrated detection filter is formed of a simple commercial floating plastic sheet Roscolux (Supergel #19: R19 Fire) inserted between the OPD and the fluidic chamber. The basic structure of an OPD is an organic heterojunction constituted of an electron donor (D) and an electron acceptor (A) sandwiched between metallic and transparent electrodes. In our system, the choice of D and A materials is fixed by algae maximum luminescence emission, e.g. 680 nm. We choose the Poly[[4,8-bis[(2-ethylhexyl)oxy]benzo[1,2-b:4,5-b']dithiophene-2,6-diyl][3-fluoro-2-[(2 ethylhexyl)carbonyl]thieno[3,4-b]thiophenediyl]] (PTB7) as electron donor since this material has already shown high photovoltaic performances, a power conversion efficiency of 7.4% (Liang 2010) and exhibited strong light harvesting between 350 and 750 nm, corresponding to the maximum chlorophyll emission. In our devices, contrary to what is usually chosen in organic solar cells, PTB7 is associated with $PC_{60}BM$ ([6,6]-phenyl-(C61)-butyric acid methyl ester) instead of $PC_{70}BM$ (([6,6]-phenyl-(C71)-butyric acid methyl ester) in order to limit the OPD photo-conversion between 400 and 550 nm (Sun 2012). Glass substrates with indium tin oxide (ITO) anodes (CEC010S purchased from Praezisions Glas & Optik GmbH) were first patterned by means of photolithography and chemical etching such as to define the active area. Then the anodes are cleaned by sonication in successive baths of acetone, ethanol and isopropanol (10 minutes each). UV/ozone treatment of 10 minutes allowed the surface cleaning before the active layer deposition. PTB7 and $PC_{60}BM$ are dissolved in chlorobenzene with DIO co-solvent (3% v/v) to obtain 30 $mg.ml^{-1}$ concentration solutions with D:A mass ratio of 1.5:1. The solution was stirred overnight at 50°C. We fabricated optimized devices by spin-coating the solution at 750 rpm for 60 seconds in a N_2-filled glovebox to achieve a thickness of 180 nm. Finally, a 100 nm aluminum electrode is evaporated on top of the bulk heterojunction. At the end, devices with a 19.6 mm^2

photosensitive area size (adjusted to fluidic chambers) were encapsulated by a cavity cover glass and sealed with epoxy adhesive.

2.5. Bioassays

The green microalga *Chlamydomonas reinhardtii* (CC-125) (Cr) is obtained from Ecotoxicology of Aquatic Microorganisms Laboratory from the Quebecker "Département des Sciences Biologiques (GRIL – TOXEN, Université du Québec, Montréal, Canada). *Pseudokirchneriella subcapitata* (Ps) and *Chlorella vulgaris* (Cv) are obtained from the French "Laboratoire d'Ecologie des Hydrosystèmes Naturels et Anthropisés" (LHENA, Université Claude Bernard, Lyon France). Cr is cultivated in 200 mL Erlenmeyer flasks at 25°C on mineral, liquid high salt medium (HSM) (Sueoka 1960) with pH 6.9 ± 0.1 and Ps and Cv in Lefebvre-Czarda medium (Ionescu 2006) with pH 7.0 ± 0.2. The cultures are aerated with the atmospheric air containing 2.5% (v/v) CO_2, which is passed through a bacteriological filter, and illuminated by white light with irradiance of 30 μE/m^2.s. The algal cell growth is synchronized by alternating light and dark periods (L/D – 14/10 h). Media and flasks are autoclaved (120°C, 1.5 bar, 20 min) before inoculation and algal solutions are transplanted once a month under sterile conditions. Experiments are conducted with cells in the exponential growth phase. Two algae solutions are studied with 1×10^6 and 6×10^6 cells/mL, noted C_1 and C_6 respectively, to evaluate the detection properties of the electrochemical and optical sensors according to cell density. To obtain the C_6 concentration, 6 mL of initial algal suspension in the exponential growth phase, C_1, is centrifuged at 800 g and re-suspended in 1mL of the culture medium. The cells count is carried out by the Fast Read 102® (Gunetti 2012), which is a plastic slide that allows the simultaneous reading of 10 chambers with a microscope.

3. Results and discussion

3.1. Electrochemical sensor validation

Following the microtechnological process, electrochemical characterization is conducted to validate the sensor. First, platinum thin layers were studied in a 0.1 M H_2SO_4 solution to compare the typical oxidative and reduction peaks during the cyclic voltammetry to the bare platinum reference curve. As previously demonstrated (Christophe 2013), cyclic voltammograms representative of polycrystalline platinum were found (result not shown).

As described in the technical part 2.3, the functionalization of the microelectrodes is made post process: AgCl is formed as the reference electrode from a thick electroplated silver layer, and the collection surface of the working electrode is increased thanks to 3D PtBl deposit.

As the main chemical specie to be detected here is dissolved oxygen, we characterize the three-electrodes ElecCell devices with saturated, aerated and desaerated oxygen solutions at room temperature. Reduction current is observed from -0.7 V as expected (Tsopela 2014). Future oxygen

measurements related to algae photosynthesis are performed by chrono-amperometry at -0.8 V to guarantee the selective monitoring of oxygen on platinum electrode. As described previously (Tsopela 2016), for herbicide detection using bio-electrochemical sensors, measurements are conducted by switching the light off and on to be able to determine: (i) the number of the active algae by the respiration slope during the dark period, (ii) the photosynthesis activity by monitoring the slope of the oxygen production during the light period. As those values are respectively estimated from the slopes of the on/off curves, 30 seconds for each period is found to be the sufficient and optimal time to obtain a fast sensing monitoring system. In this case, the integrated AgCl reference electrode is clearly stable enough for reliable measurements (see section 2.3).

As electrochemical microcells (ElecCell) constitute very sensitive devices, one of the first requirements before toxicity measurements is to define the sensor optimum operating conditions. In fact, dissolved oxygen detection may be modified by temperature variations induced by LED lighting since oxygen diffusion coefficient is affected by temperature. Thus, oxygen variation slope versus LED intensity is studied for three fluidic chamber fillings: HSM pristine solution, C_1 *Chlamydomonas reinhardtii* in HSM, and C_6 *Chlamydomonas reinhardtii* in HSM (Fig. 2). Table 1 (see supplementary information) represents the temperature enhancement regarding the LED luminance in LOC measurement configuration. Temperature variations as high as 8.8°C have been determined, in the top of the microfluidic chamber (i.e. opposite fluidic platform side regarding LED position) between light off and light on for LED maximum luminance of 7468 cd/m^2.

Since the LED used for photosynthesis is stuck to the LOC, the fluidic chamber is heated from 290 cd/m^2 incident lighting and lead to O_2 diffusion monitored by the electrochemical microcell even in HSM solution for 700 cd/m^2 (see inset Fig. 2). Finally, optimal LED luminance value chosen in order to avoid sensor transduction alteration is estimated to 290 cd/m^2. This latest value is fixed for all toxicity assays performed by chrono-amperometry thereafter.

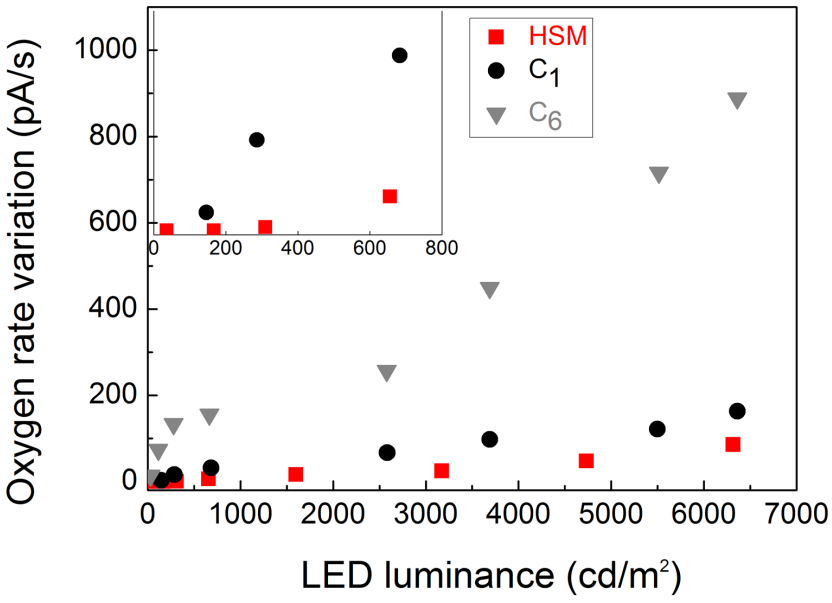

Figure 2: O_2 rate variation versus LED intensity for three fluidic chamber fillings: HSM pristine solution (red square), C_1 Chlamydomonas reinhardtii in HSM (black circle), and C_6 Chlamydomonas reinhardtii in HSM (gray triangle). Inset, zoom for HSM pristine solution and C1 in HSM in the range 0 - 800 cd/m² LED intensity.

3.2. Optical sensor validation.

For the photodiode integration in the proposed system the prerequisite are the following: (i) high external responsivity matching with biosensor emission spectra, (ii) high specific detectivity which characterizes the capability to detect the weakest light signal, (iii) output signal must be linearly proportional to the input optical signal and (iv) a device size, i.e. photon collection area, fitted on the microfluidic chambers design. Here, photodiode response time does not constitute a critical parameter for algae fluorescence measurements since in our case (continuous fluorescence monitoring) fast dynamic response is not required. In this field, OPD constitute a promising alternative to silicon-based photodetectors since they offer the ability to be processed directly on the LOC platform as close as possible to the algae. Moreover, they present high sensitivity in visible wavelength range, low dark current and are cheap to manufacture (Kielar 2016). The responsivity R and specific detectivity D* of the OPD are depicted in Figure 3. The OPD characterization has been performed at 0 and -2 V. This OPD display a significant response in terms of responsivity and detectivity between 550 and 750 nm. At 680 nm, the wavelength corresponding to chlorophyll maximum emission, the OPD responsivity is 0.38 and 0.5 A/W for 0 and -2 V bias respectively, which is close to the values reported for standard commercial photodiodes. The specific detectivity shows a maximum for the unbiased device at 10^{12} cm.Hz$^{1/2}$/W.

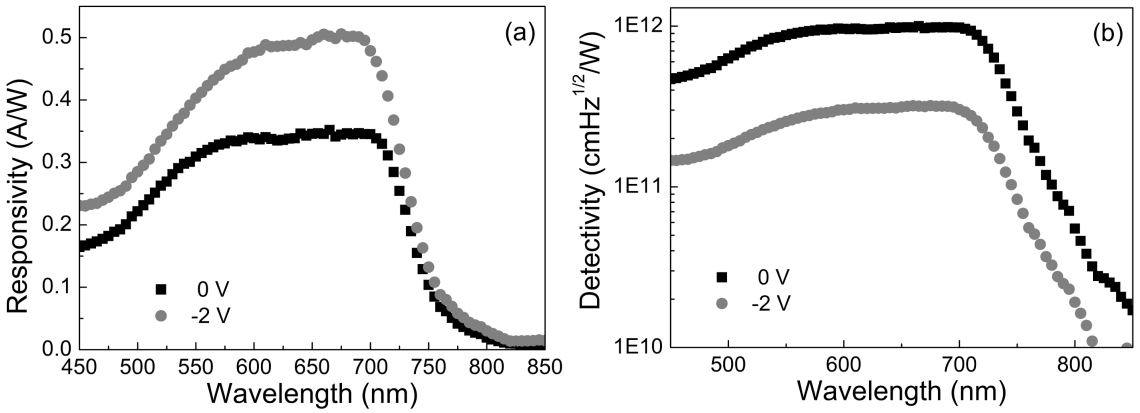

Figure 3: Responsivity (a) and detectivity (b) of the developed organic photodetector.

We followed the evolution of detectivity D* for the devices developed here according to their active area from 3 to 19.6 mm². We have noticed no significant changes in those performances (not shown). This result leads to the choice of the biggest device in order to collect the maximum of the biosensor emission. Considering that the expected algae fluorescence will be very weak, the focus is on the OPD detectivity rather than on its sensitivity. As seen in the Figure 3.b, applying a reverse bias subsequently lowers D* values. The reason for this is the rising dark current with voltage in PTB7/PC_{60}BM

photodiodes. So, in order to enhance the sensor detection range, further micro-algae fluorescence measurements will be realized at a "zero volt" bias.

Experimental data of photocurrent versus intensity of the incident light at 650 nm, for the device studied, is shown in Figure 4. There should be a linear dependence with respect to incident light intensity, at 0 V and it is verified for at least 4 orders of magnitude. The lowest detectable light intensity is 3.3 nW/cm^2, which is consistent with the fluorescence signal measured for algae in growth phase (in culture medium) with a 2600 cd/m^2 blue LED.

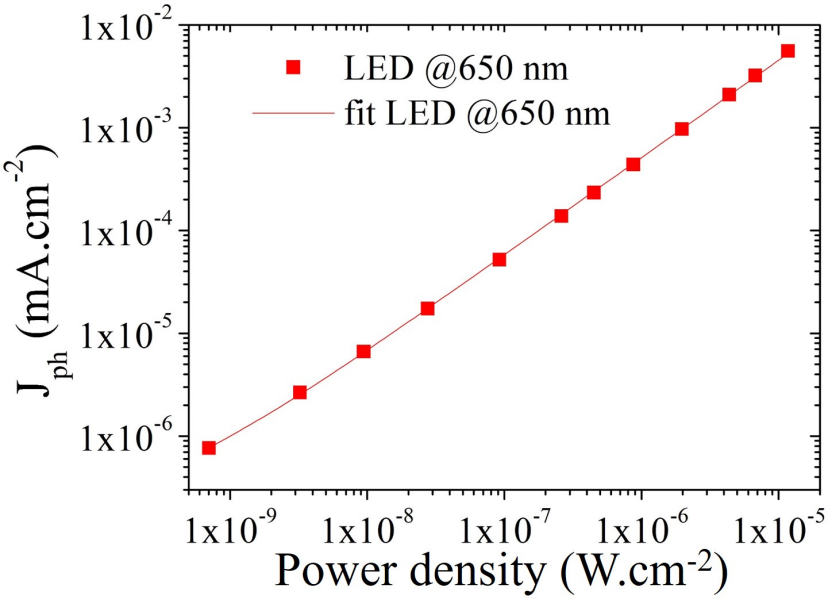

Figure 4: Photocurrent density as a function of the light intensity at 650 nm, the minimum range is equivalent to algae fluorescence.

In order to assess our optical sensor response versus algae cells density (the three algae strains are evaluated), we compare algae fluorescence signal obtained on the two algae solutions C_1 and C_6 without pollutant. The signal is recorded continuously (see Fig.S.3 supplementary information) at room temperature with the developped OPD. The measurements consist in realizing cycles of darkness and light of one minute each repeated three times for two LED intensities, 2600 and 6350 cd/m^2 respectively (2600 cd/m^2 corresponding to the lowest LED luminance allowing flurorescence signal measurement with our system, and 6350 cd/m^2 to the value used by other groups in similar sensing platforms (Lefèvre 2012)). As expected, for algae suspension from the culture C_1, photocurrent enhancement is less pronounced than for the C_6 samples, as shown on Figure 5. These signals are exacerbated when using 6350 cd/m^2 blue light as excitation source, which demonstrated a highest level of fluorescence variation between C_1 and C_6, especially for Cr and Ps micro-algae. Since, maximum photocurrent values are recorded with C_6 solutions of Cr and Ps for 6350 cd/m^2 LED lighting, further measurements involving optical sensor will be carried out, under those experimental conditions in terms of algae strains, concentration and LED luminance.

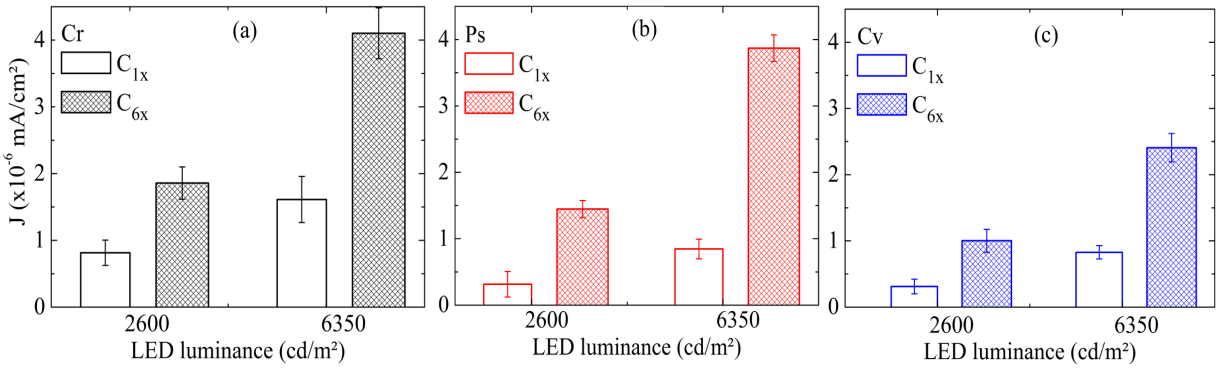

Figure 5: OPD current density monitored for three algae strains, (a) CR, (b) PS and (c) CV pristine solutions C_1 and concentrated ones C_2 for two LED intensities, 2600 cd/m² and 6350 cd/m².

3. 3. Herbicide detection using dual microsensors

To validate and compare the microsystem sensors in the presence of a pollutant, we studied the inhibition of photosynthetic activity in the presence of Diuron herbicide. Indeed, Diuron herbicide is well known to have an effect on PSII leading to an immediate impact upon chlorophyll A fluorescence yield together with O_2 production inhibition (Govindjee 1995). Two different algae solutions, C_1 and C_6, are set without and with pesticide (Diuron, *Sigma-Aldrich*, 98% purity). The pesticides concentrations were prepared in the 0 – 1 μM range to fit with environmental application.

Diuron is dissolved in ethanol (ethanol, HPLC grade, *Fischer Scientific*, 99,99 % purity) due to its low solubility in water (42 mg L^{-1} at 20°C). In turn, the nominal concentrations of each solution tested were obtained by dilution of the stock solution in culture medium. Ethanol solutions containing Diuron are mixed with algal test solutions re-suspended in culture medium in order to prepare final solutions of various Diuron concentrations (from 0 to 1 μM). Samples to be measured are then injected in the detection chambers with a simple syringe for electrochemical and optical monitoring since the microfluidic structure hydrophilic properties prevent from the use of a micro-pump.

The optical part of the biosensor is first tested in the presence of this herbicide for Cr and Ps algae strains. After a contamination time of 15 minutes, the algae fluorescence rate is detected according to the procedure described above (section 3.2). Fluorescence variations are expressed as a percentage given by the equation displayed by A. Gosset *et al*. (Gosset 2018):

$$\mathrm{FE}(\%) = \frac{Fs - Fc}{Fs} \mathrm{x}100$$

where FE is the fluorescence enhancement (in %), Fs is the fluorescence signal acquired for algae exposed to Diuron (in mA/cm²), and Fc the fluorescence signal for control algae (in mA/cm²).

Figure 6.a illustrates the fluorescence signal changes as a result of herbicide addition: the two algae appeared to be sensitive to Diuron exposure. An increase of these signals with the concentration of herbicide is observed. By far, for optical sensing, the most sensitive specie is Ps with an estimated early Diuron detection of 10 nM (20 nM for Cr).

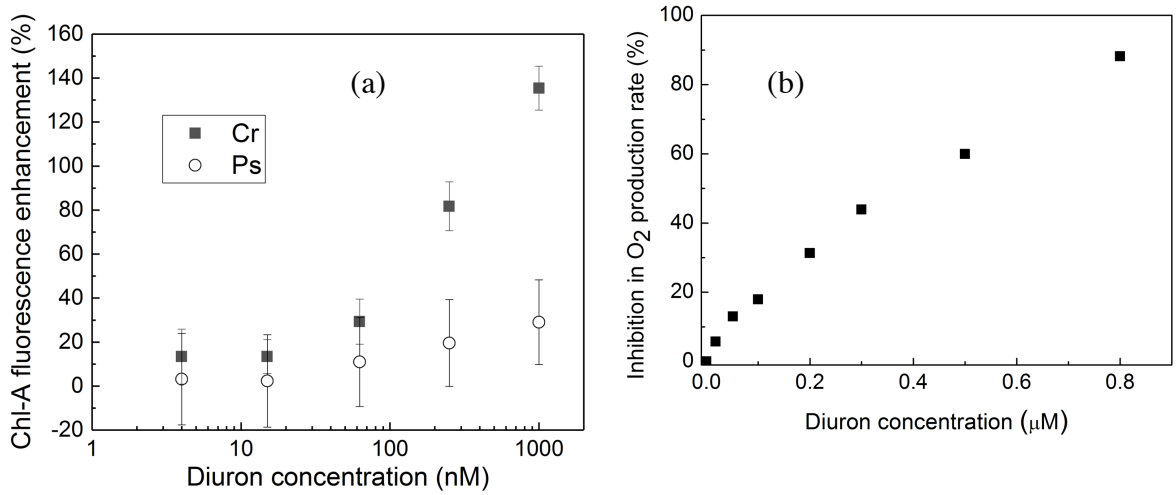

Figure 6: a) Optical biosensor response curves for two algae strains (Cr and Ps), C_6 solutions, (b) Impact of Diuron concentration on Cr O_2 production rate (C_1 solution).

A good correlation is obtained between those dose-response curves and those displayed by A. Gosset *et al*. (2018) performed on the same microalgae strains. The main advantage of the optical sensor studied here is its limit of detection which is of the order of some tens of nanomoles, similar to the LOD determined by F. Lefevre *et al*. (2012) in the same kind of systems using OLED and OPD. At first glance, this result is due to position-related optical devices in close proximity to the fluidic chamber containing the algae.Furthermore, these authors stated that their system was more sensitive than the commercial equipment Handy-PEA (Advanced Continuous Excitation Chlorophyll Fluorometer).

As described in the 3.1 part, dark and light periods were applied on an algae solution containing different pollutant concentrations. First of all, the slope of the oxygen reduction curve, obtained by chrono-amperometry technique, leads to the production of oxygen by algae (minus the respiration) when the light is on. To be able to compare each slope value versus pollutant concentration, we have to estimate very precisely the quantity of active algae responsible of the photosynthesis process, which can be different from the total number of algae obtained with a classical cell counter. For this purpose, we monitor the respiration slope during the dark period to determine the equivalent number of "alive" algae before switching the light on for the photosynthesis process. In fact, it is assumed that pollutants have no effect on the respiration phase. We use this quantification and mathematical treatment to determine the oxygen production rate versus Diuron concentration in different solutions added to algae culture. Linear response is observed (Fig. 6.b) in a large range of herbicide concentration (0.1 to 1 μM), and Diuron can be measured with a concentration range down to 0.1 nM even with the unconcentrated algae solution (C_1). In fact, no further tests using C_6 solution have been conducted as the detection properties related to the variation of oxygen production is representative enough with C_1 solution. So, we point out that for future *in-situ* use, no biosensor pre-treatment will be required to proceed to the electrochemical measurements.

The results obtained using the electrochemical microcell (ElecCell) show a large sensitivity (92% O_2 inhibition/μM) for Diuron detection over an extensive range, compatible with legal acceptable

concentrations in the frame of environmental analysis. Compared to previous works (Tsopela 2014, 2016) a linear variation is found for the highest Diuron concentrations (> 0.1 M) whereas an enhanced inhibition is evidenced for the lowest ones (< 0.1 M). Since amperometric response of the PtBl ultra-micro-electrode array is known to be linear, such phenomenon should be related to the *Chlamydomonas reinhardtii* micro-algae metabolism. Indeed, as previously discussed, we are analyzing a low algae concentration solution in order to estimate the possibility of working easily with our system. Therefore, when we look at the influence of Diuron on the photosynthetic activity of algae, the inhibitory effect is visible very early on the response curve, *i.e.* for very low concentrations of pollutant. This effect is increased tenfold by the fact that we work in micro-volume. This is expressed by a slope variation on the response curve (Fig. 6), as the Diuron concentration increases, showing a progressive saturation of the detection. It can therefore be seen that at a concentration of approximately 1 µM, the inhibition rate on such a low algae solution is already close to 100%.

The combined sensors presented in this paper demonstrate their ability to be used as an indicator of the photosynthetic activity of micro-algae biosensors, and highlight a couple method of herbicide assay. If the biological element studied is the same for the two sensors, the physiological parameters and transduction signals monitored differs. The detection limit, estimated from electrochemical measurements is a hundred times greater than that obtained with the optical sensor in the same fluidic platform. These discrepancies may stem from three factors including the nature of the measured physiological parameters (combined with two types of signal transduction), the difference in the algal concentration used for toxicity assays and the sensors sensitivity. Indeed, when using optical detection, the recorded signal consists in raw photocurrent density which has not undergone either amplification or signal processing. So, although this paper relates the coupled herbicide dual-detection with state-of-the-art devices, significant improvements will be obtained by further integration of the optical part of this system combined with signal processing. In addition, it should allow working with C_i solution for both detection principle (electrochemical/optical), namely without any biosensor pre-treatment, as it is already the case with the electrochemical sensor.

Another important outcome lies here in the ability to achieve pollutant selectivity, which is very difficult to obtain by using a single transduction system. Since chlorophyll A fluorescence is almost entirely due to Photosystem II (PSII) function targeted by several classes of herbicides (Diuron, diazines, triazine, phenols…) (Giardi 2003), the dual-sensor proposed should provide a way to discriminate some toxic chemical species.

Conclusion

A portable lab-on-chip device is developed for water toxicity environmental analysis and more especially herbicide detection. In order to provide complementary analysis, a dual sensor platform is implemented while considering both electrochemical optical detections. As a result, developing a new

fluidic packaging technology based on the use of dry film resist (DFR), three-electrode electrochemical microcells (ElecCell) and an organic photodetectors (OPD) lead, in a functional way, to a DFR-LOC fully adapted to liquid phase analysis. Demonstration is performed through the study of algal photosynthetic metabolisms by using three different algae, i.e. *Chlamydomonas reinhardtii*, *Pseudokirchneriella subcapitata* and *Chlorella vulgaris*, and dealing with Diuron herbicide. Thus, the Diuron concentration increase is found to be responsible for an algal oxygen production inhibition as well as an algal red fluorescence enhancement. Finally, it is demonstrated that (i) the ElecCell and LED/OPD microsensor technologies are successfully adapted to the analysis of algae metabolisms, and (ii) that the associated DFR-LOC device is fully adapted to the electrochemical/optical dual detection for on-site pollutant analysis, i.e. without sample pre-treatment. Fully optical integration, that involves micro-cavity OLED as excitation light and OPD as detection device, is under progress. It will increase the optical sensor sensitivity. Further works will therefore imply the development of multi-algae/multi-sensor lab-on chip in order to deal with the selective detection of different pollutants, i.e. different herbicides in a frame of a "plug-and-play" system for water analysis.

Acknowledgement

The authors would like to thank the French "Agence nationale de la Recherche" (ANR, project DOLFIN, n°ANR-13-JS03-0005-01) and the French "Fonds France-Canada pour la Recherche" (FFCR) for financing the project. Furthermore, microfabrication procedure was partly supported by the French RENATECH network.

References

- Arduini F., Cinti S., Scognamiglio V., Moscone D., Palleschi G., 2017, Analytica Chimica Acta, , 959 15-42.
- Brayner R., Couté A., Livage J., Perrette C., Sicard C., 2011, Analytical and Bioanalytical Chemistry, 401, 581–597.
- Christophe C., Sékli Belaïdi F., Launay J., Gros P., Questel E., Temple-Boyer P., 2013, Sensors and Actuators, B177 350-356.
- Fernandez-Jaramillo A.A., Duarte-Galvan C., Contreras-Medina L. M., Torres-Pacheco I., Romero-Troncoso R. de J., Guevara-Gonzalez R. G. and Millan-Almaraz J.R., 2012, Sensors, 12 11853-11869.
- Giardi M.T., Guzzella L., Euzet P., Rouillon R., and Esposito D., 2005, Env. Sci. Technol., 39 5378-5384.

- Gosset A., Durrieu C., Renaud L., Deman A.-L., Barbe P., Bayard R. and Chateaux J.F., 2018, Biosensors and Bioelectronic, 117, 669-677.
- Govindjee., 1995, Aust. J. Plant Physiol., 22 131–160.
- M. Gunetti, Castiglia S., Rustichelli D., Mareschi1 K., Sanavio F., Muraro, M., Signorino E., Castello L., Ferrero I. and Fagioli F., 2012, Journal of Translational Medicine, 10 112-123.
- Ionescu R.E., Abu-Rabeah K., Cosnier S., Durrieu C., Chovelon J.M., Marks R.S., 2006, Electroanal. 18 1041–1046.
- Jang A., Zou Z., Kug Lee K., Ahn C.H. and Bishop P.L., 2011, Measurement Science and Technology, 22 1-18.
- Kielar M., Dhez O., Pecastaings G., Curutchet A., and Hirsch L., 2016, Sci. Rep., 6:39201 1-11.
- Lefèvre F., Chalifour A., Yu L., Chodavarapu V., Juneau P., Izquierdo R., 2012, Lab Chip, 12 787‑793.
- Liang Y., Xu Z., Xia J., Tsai S-T., Wu Y., Li G., Ray C., Yu L., 2010, Advanced Materials, 22 E135‑E138.
- Sekli Belaidi F., Tsopela A., Salvagnac L., Ventalon V., Bedel-Pereira E., Bardinal V., Seguy I., Temple-Boyer P., Juneau P., Izquierdo R., Launay J., 2016, IEEE-NMDC, Nanotechnology Materials and Devices Conference**,** 9-12 October in Toulouse France, 2016.
- Sueoka N., 1960, Proc. Natl. Acad. Sci. USA, 46 83-91.
- Y. Sun, G. C. Welch, W. L. Leong, C. J. Takacs, G. C. Bazan, A.J. Heeger, , Nature Materials, 2012, 11, 44-48.
- Tahirbegi I.B., Ehgartner J., Sulzer P., Zieger S., Kasjanow A., Paradiso M., Strobl M., Bouwes D., Mayr T., Biosensors sand Bioelectronics, 2017, 88 188–195.
- Tsopela A., Lale A., Vanhove E., Reynes O., Seguy I., Temple-Boyer P., Juneau P., Izquierdo R., Launay J., 2014, Biosensors and Bioelectronics, 61, 290-297.
- Tsopela A., Laborde A., Salvagnac L., Ventalon V., Bedel-Pereira E., Seguy I., Temple-Boyer P., Juneau P., Izquierdo R., Launay J., 2016, Biosensors and Bioelectronics, 79, 568-573.
- Vanhove E., Tsopela A., Bouscayrol L., Desmoulins A., Launay J., Temple-Boyer P., 2013, Sensors and Actuators, B178 350-358.
- Vedrine C., Leclerc J.C., Durrieu C. and Tran-Minh C., 2003, Biosensors and Bioelectronics, 18, 457–463.

Part 2.3.

SEM images of this electrode are shown in Fig. S1.a. The silver chloride, about 4 μm thick, consists in homogenous grains with a size ranging from one to two micrometers.

Long-time stability in an electrolyte with 0.1 M chloride ions is verified for several hours for the reference electrode (see Fig. S1(b))

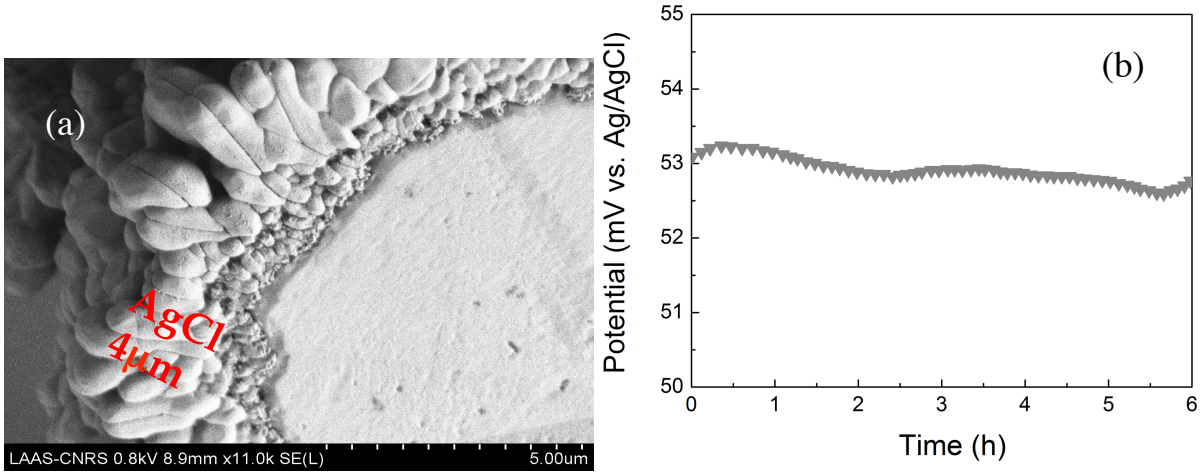

Figure S1: (a) SEM image of a silver electrode and silver/silver chloride (Ag/AgCl) interface and (b) Long-time stability of Ag/AgCl electrodes over 6 hours in an electrolyte with 0.1 M chloride ions.

Part 2.4.

The emission and excitation filters are respectively chosen to avoid overlaying of LED spurious emission and algae fluorescence signal, and to prevent excitation light to reach the OPD. The spurious LED light between 550 nm and 750 nm is of the same order of magnitude as algae fluorescence, as shown in Figure S2.

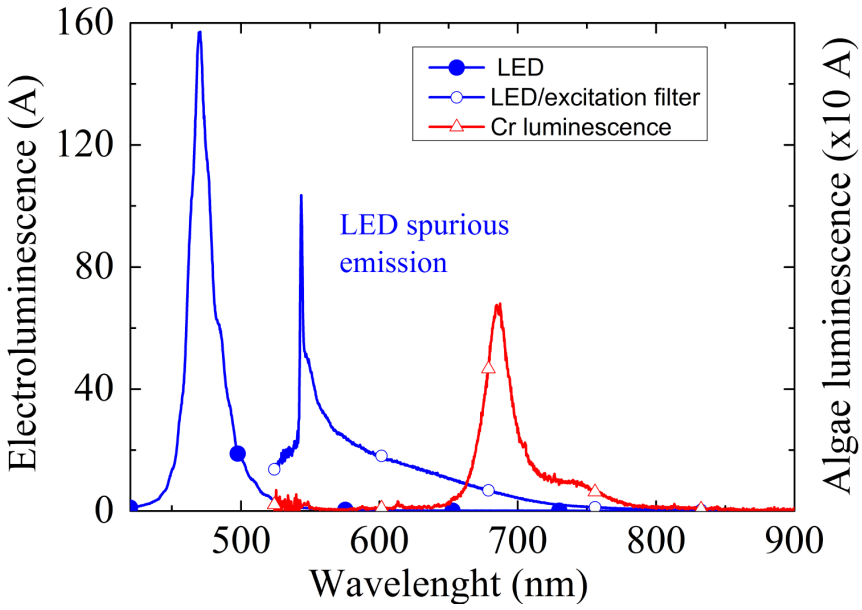

Fig. S2: Electroluminescence of blue LED before (full circle) and after filtration (empty circle) and Cr luminescence (empty triangle), spurious LED light between 550 nm and 750 nm is of the same order of magnitude as algae fluorescence.

Part 3.1

Algae fluorescence stability under operating conditions is verified (Fig. S3).

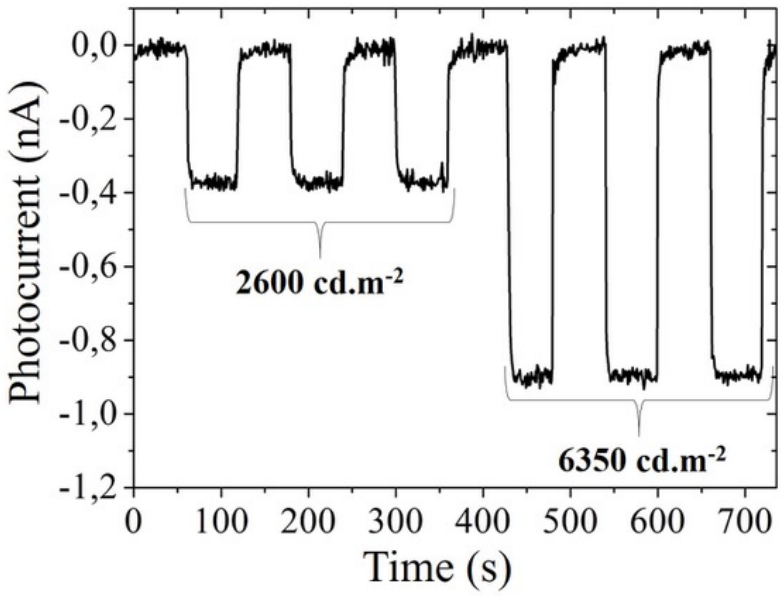

Figure S3. Evolution of photocurrent obtained for the LED luminance conditions used in this study.

Table 1: Temperature variation between light-off and light-on versus LED luminance.

LED luminance (cd/m^2)	Temperature variation between light-off and light-on (°C)
60	0
138	0
290	0.1
700	0.2
2600	1.2
3700	2.9
6350	6.4
7468	8.8